Mine Water Environ (2018) 37:505–517
DOI 10.1007/s10230-017-0490-0

TECHNICAL ARTICLE

Hydrogeological Model for Groundwater Prediction in the Shennan Mining Area, China

Peng Xie[1] · Wenping Li[1] · Dongdong Yang[1] · Junjie Jiao[1]

Received: 2 November 2016 / Accepted: 11 August 2017 / Published online: 2 September 2017

Abstract Coal mining can seriously affect groundwater systems in aquifers that overlie the coal seam, especially in dry and water-stressed areas where protection of groundwater resources is very important. Through generalization of the hydrogeological conditions and analysis of the actual groundwater flow field in a confined weathered bedrock aquifer overlying the Shennan mining area in northern Shaanxi, a hydrogeological conceptual model and numerical groundwater flow model were established. FEFLOW finite element software was used to solve the model and dynamic groundwater data were used to validate it. The study area was hydrogeologically modeled by repeatedly adjusting the parameters. The model was then used to simulate the effect of mining on the overlying aquifer based on the mining plan for the next 5 years by adjusting the quantity of water discharged, the hydrogeological parameters of the upper water-bearing zone, the characteristics of the groundwater flow field, and the predicted water balance after 5 years. The results show that the maximum drawdown could be as high as 50 m (northeast of the Zhangjiamao Mine). A cone of depression centered on the Ningtiaota, Zhangjiamao, and Hongliulin mines will be formed that will influence more than 75% of the simulation area.

Keywords Finite element · FEFLOW · Coal mining · Groundwater · Mine water

Electronic supplementary material The online version of this article (doi:10.1007/s10230-017-0490-0) contains supplementary material, which is available to authorized users.

✉ Wenping Li
wpligroup@sohu.com

[1] China University of Mining and Technology, Xuzhou, China

Introduction

While groundwater in a local or regional aquifer may threaten the safe mining of coal (Guo et al. 2015; Wu et al. 2004), the mining, and its associated dewatering can seriously impact groundwater resources (Sun et al. 2012). Comprehensive use of mine water is an urgent problem that must be addressed in the arid area of northwest China. The Shennan mining area is rich in coal resources, but more than 20 years of mining has caused a series of ecological and environmental problems (Wang et al. 2004), such as groundwater level depression (Wang and Jiang 2011), reduced river flow (Wu et al. 2014; Zhang et al. 2011), decreased flow and disappearances of springs (Chang et al. 2011; Zhang and Liu 2002), soil erosion (Ye and Zhang 2000), vegetation blight, and land desertification (Wang et al. 2008; Zhang et al. 2011). Determining the impact of future large-scale exploitation on the dynamic distribution of water resources is an important problem.

Dong et al. (2012) used FEFLOW to optimize the mine drainage capacity of China's Linnancang Coal Mine and concluded that increasing the present drainage capacity by 30% was economical and feasible. Surinaidu et al. (2014) used MODFLOW to study the net recharge of groundwater during development of the Coindavari River basin, Andhra Pradesh, India. Kim and Parizek (1997) established a groundwater flow numerical model to simulate and analyze the Noordbergum effect induced by groundwater exploitation and explained its mechanism. Because most numerical models cannot forecast uncertain information, Li et al. (2003) proposed the use of stochastic groundwater simulation to solve the problem of different scales in the mean distribution and small scale processes. Scheibe and Yabusaki (1998) simulated and analyzed the scale of the groundwater flow and the migration process with a reasonable and

practical three-dimensional groundwater flow numerical model.

The main aquifer in the Shennan mining area, which consists of weathered bedrock, adversely affects coal production. A better understanding of the interaction between this groundwater and the mine was necessary. A FEFLOW finite element model was established to analyze and predict how mining influences groundwater flow, to improve mine safety and allow reasonable utilization of the mine water.

Study Area

Location of Study Area

The Shennan mining area is located in north-central Shenmu County, Yulin City, Shaanxi Province, approximately 36 km from Shenmu County. It is composed of the three adjacent coal mines: Ningtiaota, Zhangjiamao, and Hongliulin. The study area is located north of the loess plateau in northern Shaanxi, on the southeastern margin of the Maowusu Desert, between the northern latitudes of 38°53′16″–39°07′57″ and the eastern longitudes of 110°09′33″–110°23′52″ (Fig. 1). It is a semi-arid area with an average annual rainfall of 406.18 mm and an average annual evaporation of 1774.91 mm.

Geology of the Study Area

The strata of the study area, from top to bottom, consist of aeolian sand $\left(Q_4^{eol}\right)$ and alluvial strata $\left(Q_4^{al}\right)$ of the Quaternary Holocene, Upper Pleistocene Malan Formation loess (Q_3m), Salawusu Formation silty-fine sand (Q3s), Middle Pleistocene Lishi Formation loess (Q_2l), Neogene Baode Formation

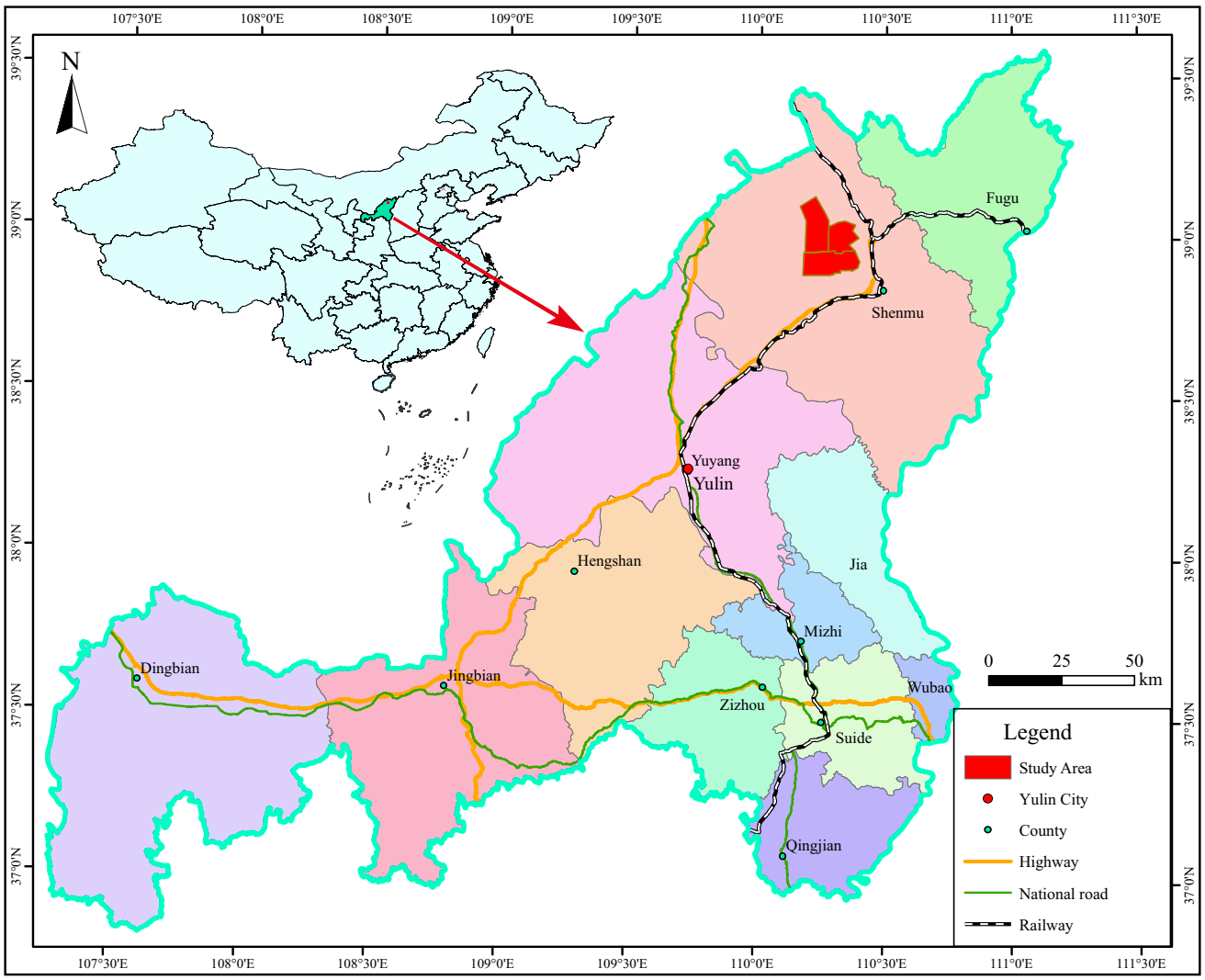

Fig. 1 Location of study area

laterite (N_2b), and the Middle Jurassic Zhiluo Formation (J_2z) and Yan'an Formation (J_2y); the coal is in the Yan'an Formation. Q_4^{al}, Q_3m, and Q_3s are mainly composed of fine sand and silt, and are discontinuous, and thin in the mining area, where they are all integrated into aeolian sand (Q_4^{eol}). The Zhiluo Formation and upper Yan'an Formation in the lower part of the Baode Formation are weathered to different degrees, and fractured, forming the main aquifer of the coal seam roof. The study area is characterized by gentle strata, a simple geological structure, and no faults (Fig. 2).

Aquifer Characteristics

The average thickness of the weathered bedrock aquifer is approximately 35 m, and the thickness decreases from west to east. West of the Hongliulin Mine and in the Ningtiaota Mine, it can be up to approximately 50 m thick, while east of the Hongliulin Mine and in the Zhangjiamao Mine, it is approximately 20 m. The weathered bedrock is mainly composed of yellow–green mudstone, silty sand, and gray sandstone. Its upper part is strongly weathered, and its weathering intensity gradually decreases with depth. Its fractures are well developed, providing good permeability and storativity.

Pumping test results for the weathered bedrock aquifer (Supplemental Table 1) revealed great spatial variability in permeability and hydraulic conductivity. The groundwater level is high in the west and low in the east, and the groundwater is mostly drained in the form of descending springs and mine drainage. The spring flow is 0.08–0.506 L s, generally 0.2 L s. The contour of the groundwater levels in September 2014 and the thickness of the weathered bedrock are shown in Fig. 3.

Groundwater Simulation Model

Aquifer Conceptualization and Discretization

As discussed above, the Baode clay layer in the upper part of the weathered bedrock aquifer can be generalized as an impermeable layer with very low permeability. The lower part of the intact and unweathered silty-fine sandstone, which has a compact texture, can be generalized as relatively impermeable. Given the variable hydraulic conductivity, a hydrogeological conceptual model of a confined aquifer with heterogeneous anisotropic fractures bearing transient flow was established. Erosion of the Kaokaowusu Gully in the northern part of the study area and Majiata Gully in the southern part of the study area has reached the weathered bedrock aquifer. Therefore, these gullies were established as the northern and southern hydraulic-head boundaries of model. To better reflect the hydrogeological characteristics of the mining area, the western boundary of the model was extended outside of the mining area, while the eastern boundary of the model coincided with the mining area's boundary. The final model covers 23.75 km from north to south and 24.75 km from east to west, with a total area of 436.31 km^2. The model, based on the three-dimensional movement of groundwater in a heterogeneous and anisotropic aquifer, is given by the partial differential equation:

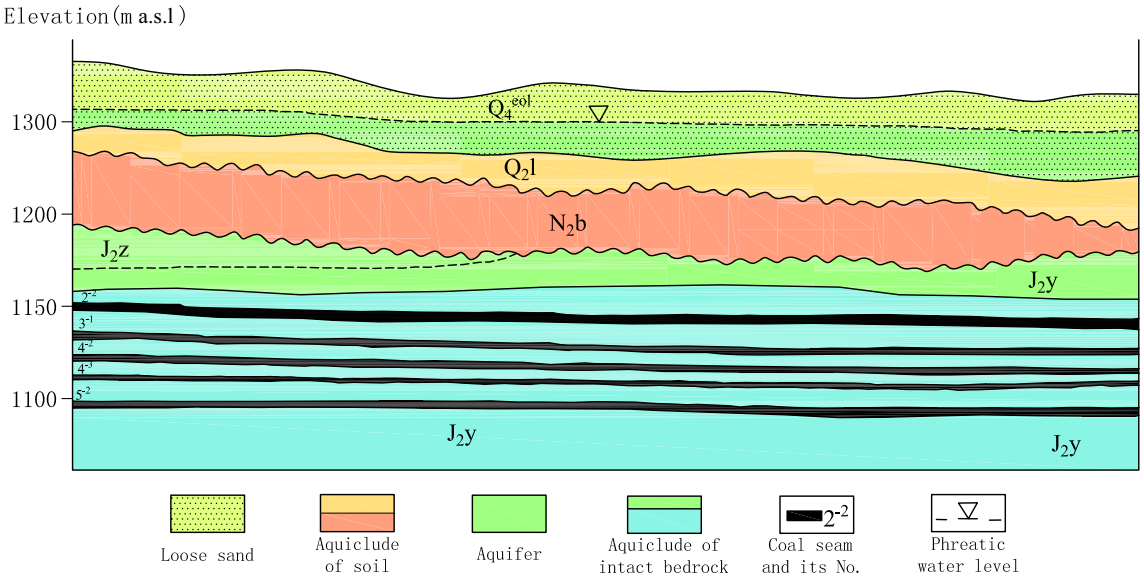

Fig. 2 Schematic stratigraphic section of the study area

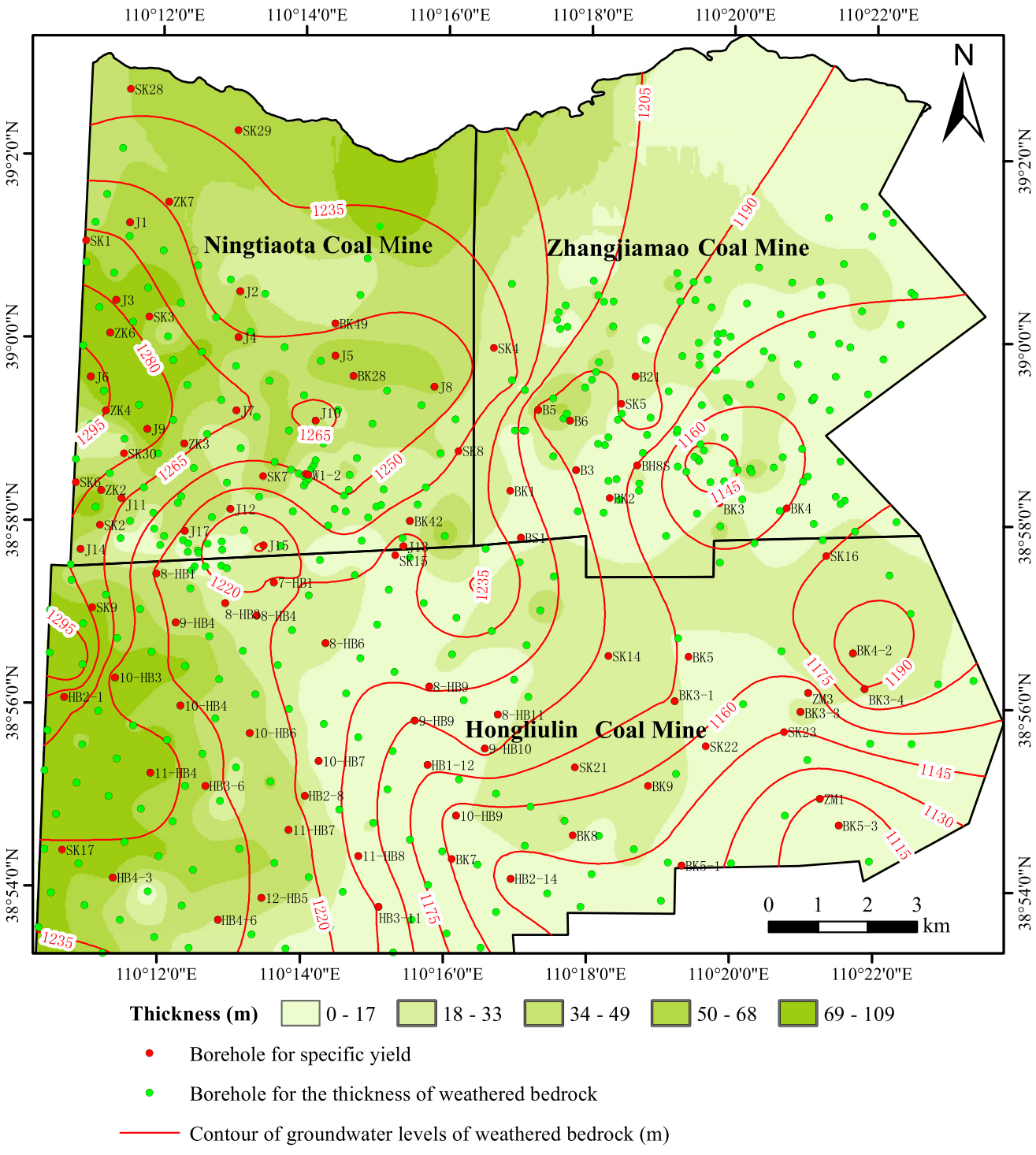

Fig. 3 Contour of groundwater levels (September, 2014) and thickness of weathered bedrock

$$\begin{cases} \frac{\partial}{\partial x}\left(K_x \frac{\partial H}{\partial x}\right) + \frac{\partial}{\partial y}\left(K_y \frac{\partial H}{\partial y}\right) + \frac{\partial}{\partial z}\left(K_z \frac{\partial H}{\partial z}\right) + \varepsilon = S_s \frac{\partial H}{\partial t} & x, y, z \in \Omega, \quad t \geqslant 0 \\ H(x,y,z)|_{t=0} = H_0 & x, y, z \in \Omega, \quad t \geqslant 0 \\ K_n \frac{\partial H}{\partial \vec{n}}\Big|_{\Gamma} = q'(x,y,z,t) & x, y, z \in \Gamma, \quad t \geqslant 0 \end{cases} \quad (1)$$

where K_x, K_y, and K_z are the hydraulic conductivity along the x, y, and z coordinate axes (L/T); H is the hydraulic head (L); t is the time (T); ε is the volume flux per unit volume representing a source/sink (1/T); S_s is the specific storage of the porous media (1/L); $\vec{n}$ is the normal vector of the boundary; q′ is the inflow or outflow volume flux from a unit area in a unit time of the second boundary condition (L/T); H_0 is the groundwater level elevation at time t = 0 (L); Ω is the scope of the model; and Γ is the fluid-flux boundary of the seepage area.

Subsequently, the finite element software FEFLOW was used to solve Eq. (1). The model was divided using a

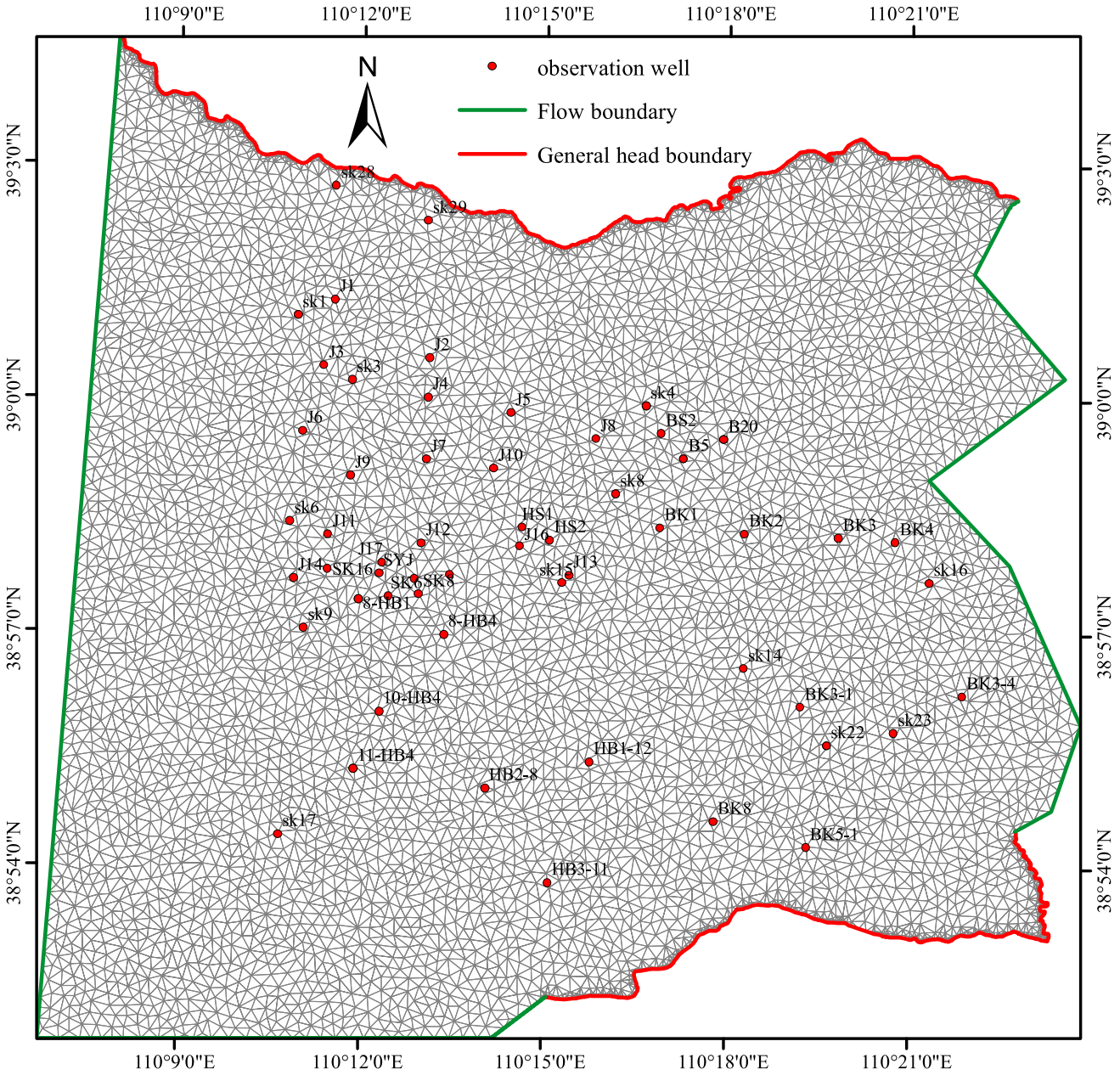

Fig. 4 Two-dimensional (2D) mesh network and boundary conditions of the model

three-dimensional triangular mesh, and an automatic refining technology was applied to areas with large hydraulic gradients, such as the Kaokaowusu and Majiata gullies. This is because the upper and lower strata of the weathered bedrock aquifer were both generalized as impermeable, and served as the upper and lower model boundaries. The model consisted of one layer and two slices, and contained 13,576 elements and 15,940 nodes in the plane (Fig. 4). Since the

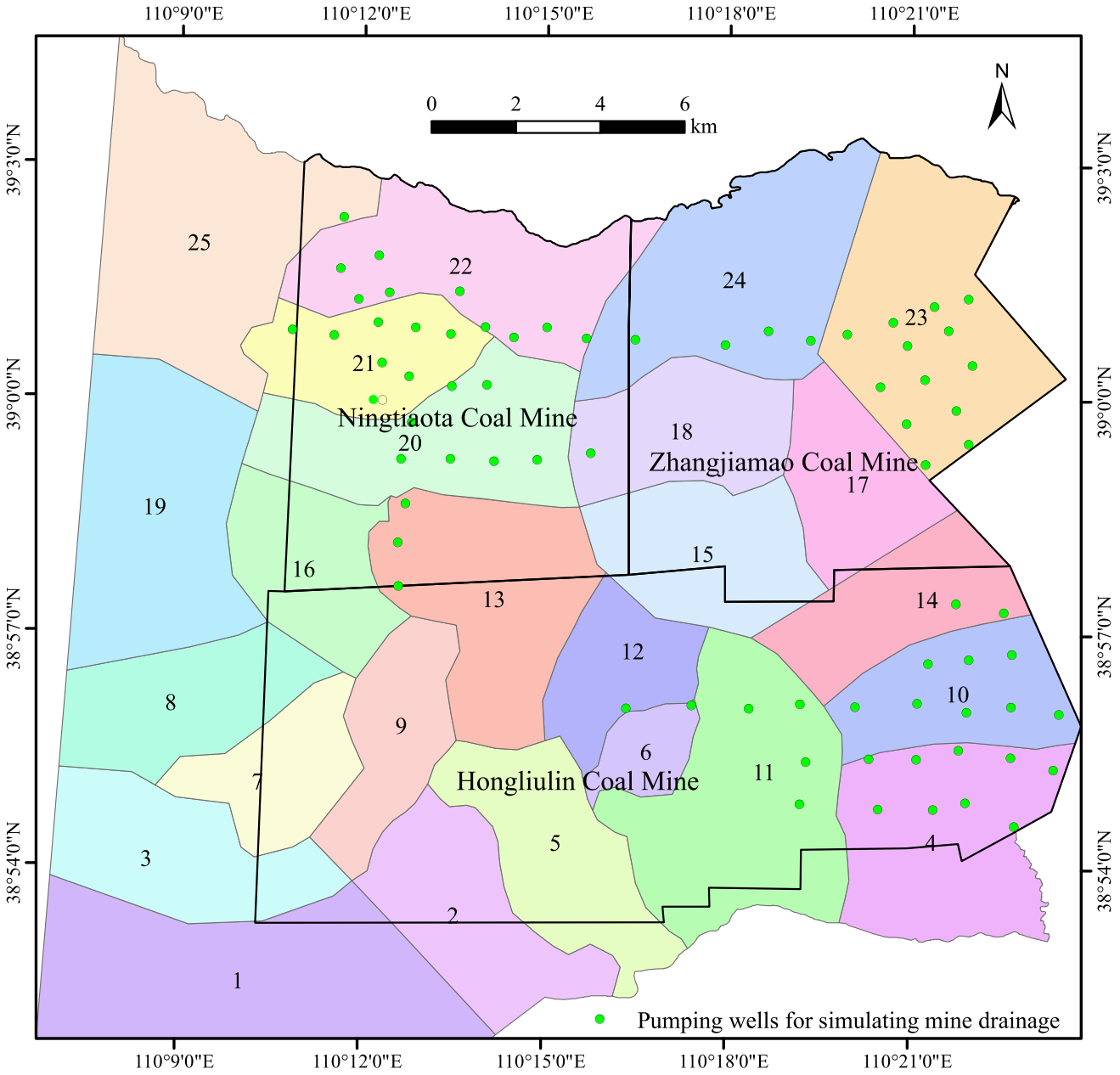

Fig. 5 Parameter zonation of numerical simulation and location of pumping wells for simulating mine drainage

Table 1 Empirical value of specific storage (S_s) for different rocks and soils (China Geological Survey 2012)

Types of soil and rock	S_s (m^{-1})	Types of soil and rock	S_s (m^{-1})
Plastic soft clay	2.0×10^{-2} to 2.6×10^{-3}	Dense sand	2×10^{-4} to 1.3×10^{-4}
Hard clay	2.6×10^{-3} to 1.3×10^{-3}	Dense sand gravel	1×10^{-4} to 4.9×10^{-5}
Medium hard clay	1.3×10^{-3} to 6.9×10^{-4}	Fractured rock	6.9×10^{-5} to 3.3×10^{-6}
Loose sand	1×10^{-3} to 4.9×10^{-4}	Relatively intact rock	$<3.3\times10^{-6}$

strata in the FEFLOW program must be continuous, the stratum thickness was set to be very small (as little as 0.01 m) for discontinuities where the formation was not continuous.

Model Parameters and Boundary Conditions

Based on an interpolation and reclassification of the hydraulic conductivity (K) and the specific yield (q) results (Supplemental Table 1) from the borehole pumping tests using ArcGIS software, and considering the characteristics of the groundwater flow field, the confined aquifer was divided into 25 zones (Fig. 5). The specific storage (S_s), referred to as "storage properties", characterizes the capacity of a confined aquifer to release groundwater. The zonation of S_s was consistent with the hydraulic conductivity, and its value is empirical (Table 1). Since the confined aquifer consisted of fractured rock, the initial value of S_s should range between 10^{-4} and 10^{-6} m^{-1}.

The aquifer limits can be described by natural or hydrological boundaries (Fig. 4). As discussed above, the gullies were generalized as hydraulic-head boundaries, with the river water level its hydraulic head value. Figure 3 shows the water level elevation contours of the weathered bedrock in September 2014. The groundwater flows from west to north,

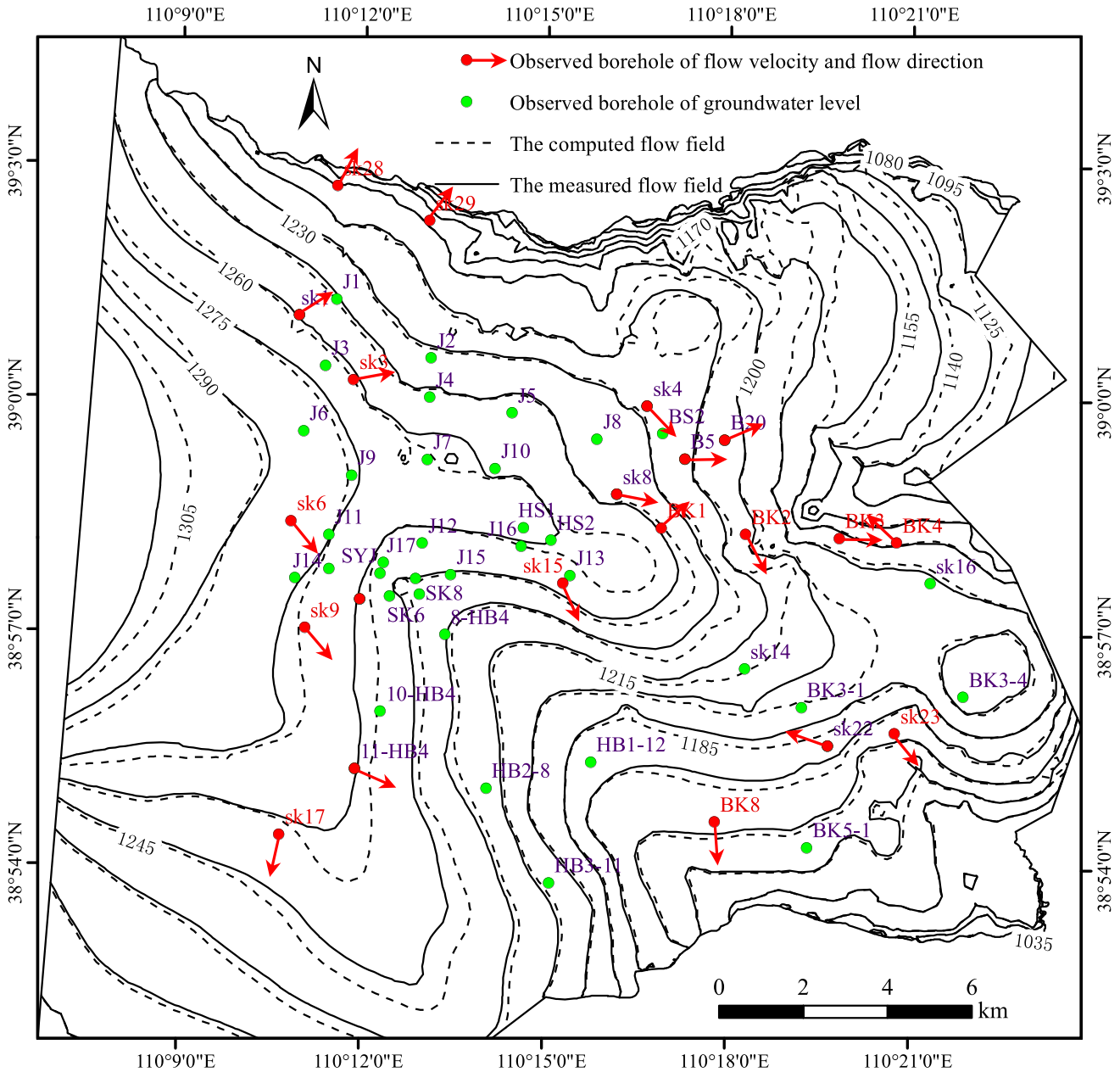

Fig. 6 Flow field comparison between simulation and observation in weathered-rock confined aquifer (30 April, 2015)

to east and south. The western and eastern boundaries of the confined aquifer of the weathered bedrock of the model were generalized to be the second type of flux boundary. The western boundary was the recharge boundary and the eastern the drainage boundary. The flux at the boundary was determined by the hydraulic gradient, the average permeability coefficient, and the thickness of the aquifer at the boundary.

When a coal seam under a weathered bedrock aquifer is mined, the aquifer will be dewatered, producing mine water inflow. In the model, wells were used throughout the model to simulate mine water inflow. A simulation was done at each node of the finite element grid and then interpolated within the finite element. The value of the nodes was close to the true value, but to get a better computed result, all pumping wells were set in the mesh nodes. The injection well was negative, and the pumping well and the mine water inflow were positive. Thirty wells were evenly distributed in the working face and goaf of the Ningtiaota Mine. The flux of each well was 524.96 m^3/day, and the total discharge was 15,748.80 m^3/day (measured value). Twenty-six wells were evenly distributed in the working face and goaf of the Hongliulin Mine. The flux of each well was 241.85 m^3/day, and the total discharge was 6,288.00 m^3/day (measured value). Seventeen wells were evenly distributed in the working face and goaf of the Zhangjiamao Mine. The flux of each well was 200.72 m^3/day, and the total discharge was 3,412.32 m^3/day (measured value). Figure 5 shows the layout of the pumping wells used to simulate the mine drainage.

Results and Discussion

Model Calibration and Validation

Observed groundwater level data from September 2014 to April 2015 (240 days in total) were used for model calibration. During this period, groundwater levels were measured every half a month. The initial flow field was determined from the observed groundwater level in September 2014 (Supplemental Table 1). By constant adjustment of the hydrogeological parameters, the dynamic changes in the groundwater level were kept as close as possible to the observation data so that the model could simulate the actual hydrogeological conditions and structural parameters.

At the end of the simulation (240 days), the simulated flow field of the confined aquifer was compared with the observed flow field (Fig. 6). The groundwater flow velocity and flow direction were measured in June 2015 by the AquaVISION Colloidal Borescope System (New Zealand AquaVISION Company; Table 2).

It can be seen from Fig. 6 that the simulated flow field agrees well with the observed flow field at the end of the simulation recognition period, and the whole flow direction is consistent with the measured flow direction of the observation borehole. Only the measured flow direction of the sk22 hole differed from the simulated flow direction, which may be due to observation error. Because the AquaVISION Colloidal Borescope System measures groundwater flow velocity and flow direction with high sensitivity based on the movement of small particles in the water, small vibrations can cause large errors. However, on the whole, the simulated and measured flows fit well. By comparing the computed flow velocity with the observed flow velocities in 20 observation wells at the end of the simulation, we learned that wells with an absolute error less than 1.0×10^{-5} m/s accounted for 65% of the total error and observation wells with an absolute error greater than 2.0×10^{-5} m/s accounted for only 10% of the total

Table 3 Error statistics between observed flow velocity and simulated flow velocity

Absolute error ($\times10^{-5}$ m/s)	≤1.0	1.0–2.0	≥2.0
Number of observation points	13	5	2
Percentage of the total (%)	65	25	10

Table 2 Observed velocity and direction of the groundwater flow

Borehole no.	Flow direction (°, azimuth)	Flow velocity (10^{-5} m/s)	Borehole no.	Flow direction (°, azimuth)	Flow velocity (10^{-5} m/s)
sk9	139.53	11.34	sk8	100.96	8.80
sk15	155.74	12.59	sk28	27.51	6.91
sk17	192.65	8.59	sk29	37.08	5.29
11-HB4	113.66	20.65	sk4	136.51	1.53
sk22	289.35	9.35	BK1	48.42	9.95
sk23	140.42	1.48	BK2	152.76	3.58
BK8	175.92	5.13	BK3	90.59	11.82
sk1	57.40	17.45	BK4	313.40	42.42
sk3	79.58	28.53	B5	88.99	6.26
sk6	140.94	9.02	B20	66.81	9.40

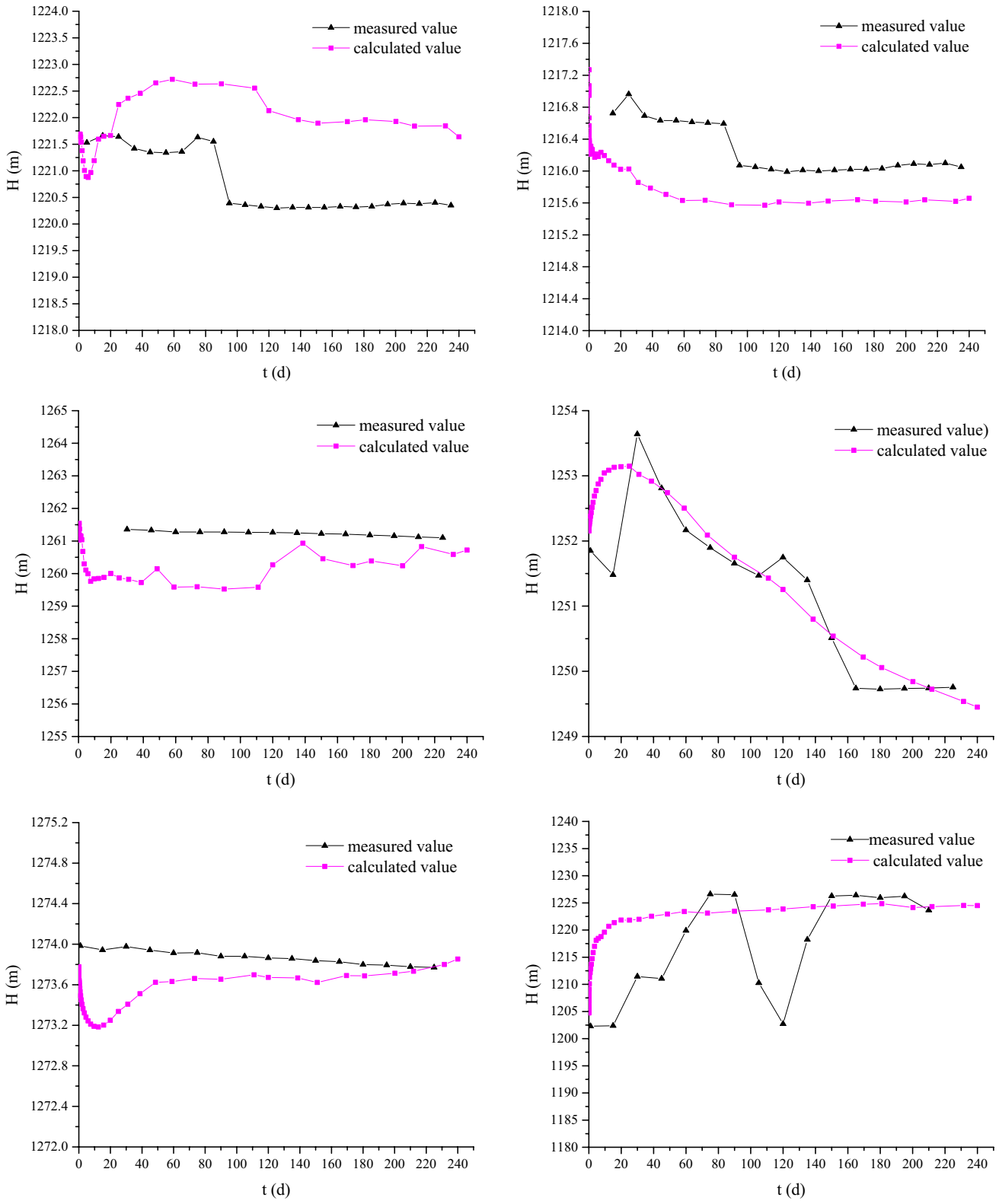

Fig. 7 Groundwater head fitting curves of some observation wells of a weathered-rock confined aquifer

(Table 3). This indicates that the model is valid and can be used to forecast future seepage. The characteristics of the flow field reflects the groundwater flow patterns of the confined aquifer. The contours of the groundwater level are affected by the main valleys. The isoline is also denser in the place where the terrain is abrupt, which is consistent with the weathered bedrock at the bottom of the valley. The groundwater of the weathered bedrock aquifer mainly drains into the valley.

The dynamic changes in the groundwater level of some representative observation wells were selected to test the simulation results; the measured and simulated groundwater levels met the convergence conditions (Fig. 7). The relative error of the fitting point was relatively small, and the fit was excellent. The groundwater head error was generally between 0.01 and 2.10 m. Borehole J4 is very close to the mine face, and the variation of the groundwater heads in the simulation period fit the trend of the simulated water level very well. This indicates that the simulation can be used to distribute the mine water discharge into a multi-port pumping well.

The sensitivity of the effect of the parameters on the model outcome was tested by varying the parameters. The aim of this sensitivity analysis was to quantify the uncertainty in the calibrated model caused by the estimation of the aquifer parameters. The uncertainty was quantified by calculating the changes in the heads caused by changes in the parameter values. The results provide a better understanding of the model's performance and indicate what data have to be collected in the field to further improve performance.

Table 4 shows the sensitivity of various parameters on simulated 2015 groundwater levels. The model was very sensitive to changes in the recharge, horizontal permeability, and vertical permeability, but less sensitive to changes in specific storage. For example, a 50% increase in recharge (approximately 132×10^6 m^3) caused an average increase in the calculated head of 66 m, and a 50% decrease in the recharge (approximately 132×10^6 m^3) caused an average decrease in the calculated head of 82 m. There were similar influences from changes in the horizontal and vertical hydraulic conductivity values, but relatively smaller changes associated with changes in

Table 4 Sensitivity effects of hydrogeological parameters on modeled groundwater levels in 2015

	Recharge		Horizontal hydraulic conductivity ($K_h = 14.00\times10^{-6}$ m/s)		Vertical hydraulic conductivity ($K_v = 1.92\times10^{-6}$ m/s)		Specific storage ($S_s = 5.2\times10^{-5}$ m^{-1})	
	+50% ($\approx132\times10^6$ m^3)	−50% ($\approx132\times10^6$ m^3)	$K_h\times10$	$K_h\times10^{-1}$	$K_v\times10$	$K_v\times10^{-1}$	$S_s\times10$	$S_s\times10^{-1}$
Variations of groundwater level (m)	+66	−82	−22	+35	+46	−33	+15	−10

+ represents an increase and – represents a decrease

Table 5 Hydrogeological parameters of each zone of the weathered-rock confined aquifer identified by the model

No.	K_x (10^{-6} m/s)	K_y (10^{-6} m/s)	K_z (10^{-6} m/s)	S_s (10^{-5} m^{-1})	No.	K_x (10^{-6} m/s)	K_y (10^{-6} m/s)	K_z (10^{-6} m/s)	S_s (10^{-5} m^{-1})
1	4.99	5.28	0.45	3.1	14	20.84	20.84	2.08	10.4
2	9.26	9.26	0.93	3.6	15	3.73	4.17	1.11	2.6
3	3.94	3.94	0.39	1.0	16	7.89	7.89	0.94	5.2
4	8.41	8.41	0.84	0.7	17	39.43	39.43	9.73	3.5
5	12.62	12.62	1.26	4.4	18	41.20	64.35	5.56	5.0
6	12.23	12.23	1.23	4.2	19	10.21	9.63	1.08	3.5
7	2.12	2.12	0.68	8.1	20	6.39	7.97	1.78	9.0
8	10.47	10.47	1.05	3.2	21	5.93	5.93	1.13	7.5
9	4.63	4.63	0.98	2.3	22	6.83	6.71	0.37	6.0
10	6.42	6.06	0.88	18.4	23	68.94	68.94	6.90	6.8
11	22.22	22.34	3.01	2.0	24	9.03	2.89	3.45	13.1
12	7.99	7.64	0.69	4.0	25	7.73	7.73	0.58	1.6
13	7.62	7.62	0.97	0.8					

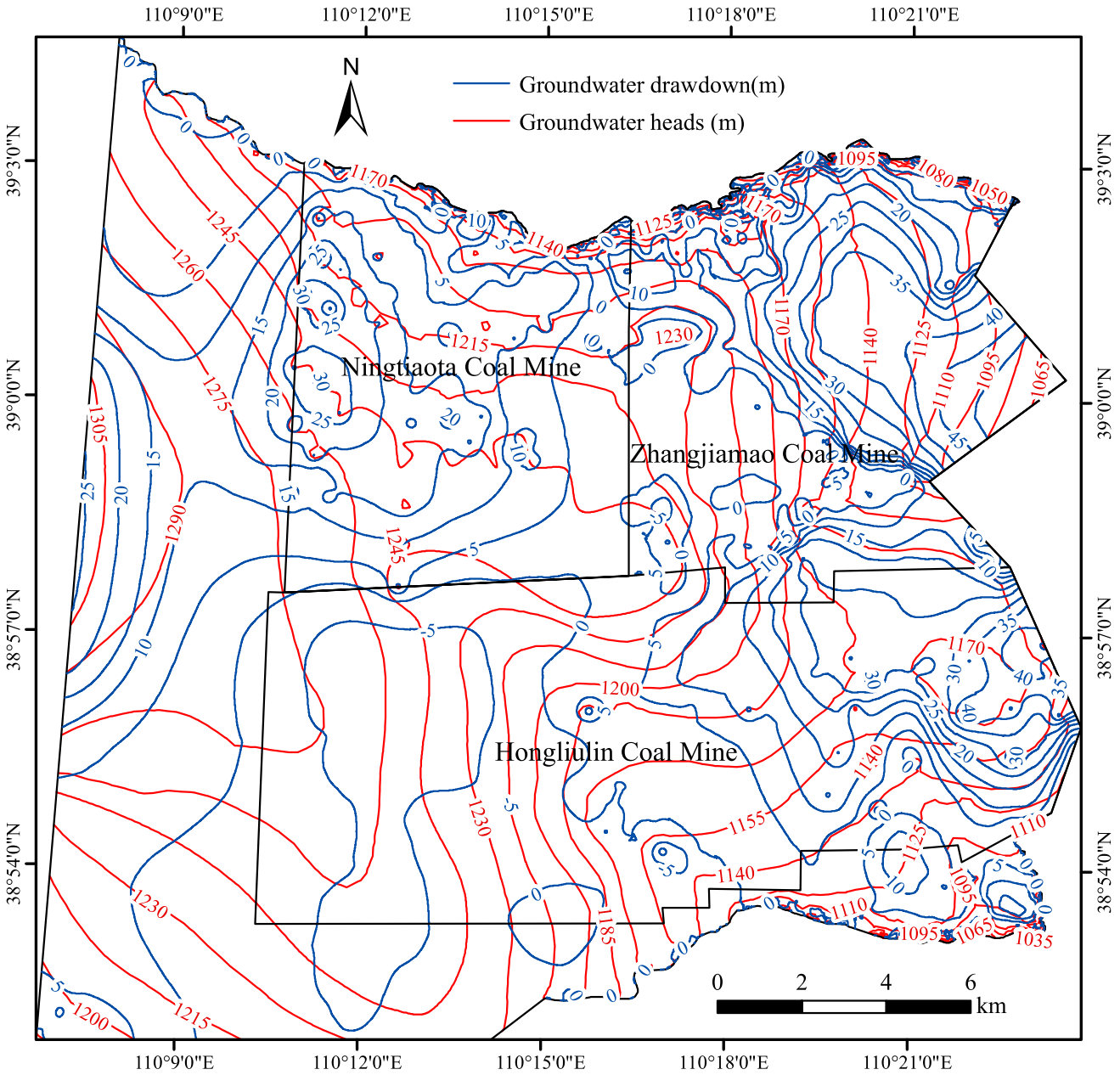

Fig. 8 Prediction of groundwater heads and drawdown contour map of weathered-rock confined aquifer at 30 April 2020 (against 30 April 2015)

specific storage. In summary, the established hydrogeological model adequately reflects the study area's actual hydrogeological characteristics. The hydrogeological parameters of each zonation are shown in Table 5.

Groundwater Budget and Model Predictions

To ensure safe exploitation, it is necessary to reduce groundwater in the upper part of the coal seam. That will greatly affect the groundwater flow field of the overlying aquifer and the distribution of the area's groundwater resources. The relationship between the groundwater level and water resource quantity and water drainage in the mining area can be quantitatively described and predicted using the numerical groundwater flow model established above. By adjusting some solution conditions, and accounting for the effect of mining on the permeability coefficient of the overlying aquifer/aquiclude, the dynamic characteristics of the groundwater flow field and groundwater balance in the overlying aquifer can be predicted and used to guide production

Table 6 Groundwater balance analysis of each mine during the model prediction period in the simulation area

Groundwater balance items	Groundwater variation of each coal mine (10^6 m^3)		
	Ningtiaota	Zhangjiamao	Hongliulin
Recharge			
Lateral recharge	419.37	329.00	487.62
Discharge			
Mine water inflow	33.21	4.40	15.22
Lateral discharge	405.53	336.45	484.87
Net inflow	−19.37	−11.85	−12.47
Average annual inflow (10^6 m^3/a)	−3.87	−2.37	−2.49

planning and water resources utilization in the area. For the short-term exploitation plan and production and domestic water demand of Shennan Mining Area in the next 5 years, the simulation forecast period will be 30 April 2015 to 30 April 2020.

The effect of coal mining on the weathered bedrock is mainly an increase in vertical hydraulic conductivity. The water conductive fracture zone that represents the mine is developed only in the working face area. Therefore, the vertical hydraulic conductivity was adjusted to ten times the horizontal hydraulic conductivity (Bian 2014). Pumping wells to simulate mine inflow were expanded to the entire mining area based on the density of the pumping wells of the model. Other parameters remained unchanged.

Figure 8 is the predicted contour map of the groundwater level and drawdown in the weathered bedrock on 30 April 2020 (compared to 30 April 2015). It can be observed that the maximum drawdown may be as high as 50 m (northeast of the Zhangjiamao Mine), which reaches the bottom of the aquifer. A cone of depression centered on the three mines has formed. The influence of the cone of depression accounts for more than 75% of the simulation area, but there is only a small impact west of the Hongliulin Mine far away from the study area.

At present, the design production capacity levels of the Ningtiaota, Zhangjiamao, and Hongliulin coal mines are 12, 8, and 12 Mt/a, and the water consumption levels are 5536, 4373, and 8607 m^3/day, respectively. The groundwater temperature of the groundwater in the aquifer is generally 3–18 °C, the pH ranges from 7.39 to 8.23, and the total hardness ranged from 25.0 to 230.2 mg/L (calculated as calcium carbonate). The mineralization of the weathered bedrock is generally 212–228 mg/L (fresh water), and the water chemistry type is generally HCO_3–Ca·Na and HCO_3–Ca·Mg. The TDS of the groundwater is less than 450 mg/L. The water meets the standards for drinking water (Ministry of Health 2006) and can be used as domestic water after disinfection. As seen in Table 6, the current average annual inflows of the coal mines are 6.64×10^6 m^3/a for Ningtiaota, 0.88×10^6 m^3/a for Zhangjiamao and 3.04×10^6 m^3/a for Hongliulin, and can supply approximately 1.82×10^4 m^3/day (3.29 times the Ningtiaota Mine's water requirement), 0.24×10^4 m^3/day (54.88% of the Zhangjiamao Mine's water demand) and 0.83×10^4 m^3/day (96.43% of the Hongliulin Mine's water demand). Thus, mine drainage water can be used for coal production and domestic water after simple treatment, which will reduce the waste of water resources and contribute to the sustainable development of mining areas.

Conclusion

A hydrogeological model based on FEFLOW finite element software was established to predict the groundwater flow field and water balance of a weathered bedrock aquifer in a mining area. The results indicate that the maximum drawdown in the next 5 years can be as high as 50 m (northeast of the Zhangjiamao Coal Mine), which reaches the bottom of the aquifer. It can therefore be inferred that the springs formed by the discharge of groundwater from the weathered bedrock aquifer may stop. The surface water may even supply groundwater in the rainy season, which will increase mine water inflow and threaten mine production security.

Mine drainage can be used for coal production and domestic water after simple treatment, which would greatly ease the area's water demand. This rational use of mine water can make a great contribution to the sustainable development of mining areas.

Acknowledgements The authors thank everyone who provided assistance for the present study. This study was jointly supported by the National Key Basic Research and Development Program of China (973 Program, Grant 2015CB251601) and the State Key Program of National Natural Science of China (Grant 41430643).

References

Bian H (2014) Numerical simulation study on the impact of water conservation under coal mining a case study of Yushen Mine in third-stage mining. Chang'an University, Xi'an **(in Chinese)**

Chang J, Li W, Li T, Du P (2011) Zonation of water resources leakage due to coal mining in Shennan mining area. Coal Geol Explor 39(5):41–45 **(in Chinese)**

China Geological Survey (2012) Handbook of hydrogeology, 2nd edn. Geological Publishing House, China, pp 128–129 **(in Chinese)**

Dong D, Sun W, Xi S (2012) Optimization of mine drainage capacity using FEFLOW for the no. 14 coal seam of China's Linnancang coal mine. Mine Water Environ 31:353–360

Guo W, Zhao J, Yin L, Li Y, Zhang B, Lu C (2015) Influences of water pressure and advance length on floor water inrush based

on mechanism of fluid–solid coupling. Electron J Geotech Eng 20(7):1947–1956

Kim JM, Parizek RR (1997) Numerical simulation of the Noordbergum effect resulting from groundwater pumping in a layered aquifer system. J Hydrol 202(1):231–243

Li SG, McLaughlin D, Liao HS (2003) A computationally practical method for stochastic groundwater modeling. Adv Water Resour 26(11):1137–1148

Ministry of Health (Ministry of Health of the People's Republic of China, Standardization Administration of the People's Republic of China) (2006) Standards for drinking water quality (GB5749-2006). Standards Press of China, Beijing **(in Chinese)**

Scheibe T, Yabusaki S (1998) Scaling of flow and transport behavior in heterogeneous groundwater systems. Adv Water Resour 22(3):223–238

Sun W, Wu Q, Dong D, Jiao J (2012) Avoiding coal–water conflicts during the development of China's large coal-producing regions. Mine Water Environ 31(1):74–78

Surinaidu L, Rao VG, Rao NS, Srinu S (2014) Hydrogeological and groundwater modeling studies to estimate the groundwater inflows into the coal mines at different mine development stages using MODFLOW, Andhra Pradesh, India. Water Resour Ind 7–8:49–65

Wang H, Jiang Z (2011) Analysis of groundwater resources and mining effect in Shennan mining area of China. Shaanxi Coal 30(5):1–4 **(in Chinese)**

Wang W, Li Z, Zhang P (2004) Environmental disaster issues induced by coal exploitation in Shenfu-Dongsheng coal field. Chin J Ecol 23(1):34–38 **(in Chinese)**

Wang L, Wei S, Wang Q (2008) Effect of coal exploitation on groundwater and vegetation in the Yushenfu coal mine. J Chin Coal Soc 33(12):1408–1414 **(in Chinese)**

Wu Q, Wang M, Wu X (2004) Investigations of groundwater bursting into coalmine seam floors from fault zones. Int J Rock Mech Min Sci 41(4):557–571

Wu X, Li H, Dong Y, Liu T (2014) Quantitative identification of coal mining and other human activities on river runoff in northern Shaanxi region. Acta Sci Circum 34(3):772–780 **(in Chinese)**

Ye G, Zhang L (2000) The main hydro-engineering-environmental–geological problems arose from the exploitation of coal resource in Yu-Shen-Fu mine area of northern Shaanxi and their prevention measures. J Eng Geol 8(4):446–455 **(in Chinese)**

Zhang F, Liu W (2002) A numerical simulation on the influence of underground water flow regime caused by coal mining—a case study in Daliuta, Shenfu mining area. J Safety Environ 2(4):30–33 **(in Chinese)**

Zhang S, Ma C, Zhang L (2011) The regulators of runoff of the Ulan Moron River in the Daliuta mine area: the effects of mine coal. Acta Sci Circum 31(4):889–896 **(in Chinese)**